

CaSR signaling down-regulates AQP2 expression via a novel microRNA pathway in pendrin and NaCl cotransporter knockout mice

Marianna Ranieri,^{*} Kamyar Zahedi,^{†,‡,§} Grazia Tamma,^{*,¶} Mariangela Centrone,^{*} Annarita Di Mise,^{*} Manoocher Soleimani,^{†,‡,§} and Giovanna Valenti^{*,¶,||,1}

^{*}Department of Biosciences, Biotechnologies, and Biopharmaceutics and ^{||}Centre of Excellence in Comparative Genomics, University of Bari, Bari, Italy; [†]Research Services, Veterans Affairs Medical Center, Cincinnati, Ohio, USA; [‡]Department of Medicine and [§]Center on Genetics of Transport and Epithelial Biology, University of Cincinnati, Cincinnati, Ohio, USA; and [¶]Istituto Nazionale di Biostrutture e Biosistemi, Rome, Italy

ABSTRACT: High concentrations of urinary calcium counteract vasopressin action *via* the activation of the calcium-sensing receptor (CaSR) that is expressed in the luminal membrane of collecting duct cells, which impairs the trafficking of aquaporin-2 (AQP2). Pendrin/NaCl cotransporter double-knockout (dKO) mice display significant calcium wasting and develop severe volume depletion, despite increased circulating vasopressin levels. We hypothesized that the CaSR-mediated impairment of AQP2 expression/trafficking underlies vasopressin resistance in dKO mice. Compared with wild-type mice, in renal inner medulla, dKO mice had reduced total AQP2 sensitive to proteasome inhibitors, higher levels of AQP2-pS261, ubiquitinated AQP2, and p38-MAPK, an enzyme that is activated by CaSR signaling and known to phosphorylate AQP2 at Ser261. CaSR inhibition with the calcilytic NPS2143 reversed these effects, which indicates that CaSR mediates the up-regulation of AQP2-pS261, ubiquitination, and degradation. Of note, dKO mice demonstrated significantly higher AQP2-targeting miRNA-137 that was reduced upon CaSR inhibition, supporting a critical role for CaSR in the down-regulation of AQP2 expression. Our data indicate that CaSR signaling reduces AQP2 abundance both *via* AQP2-targeting miRNA-137 and the p38-MAPK/AQP2-pS261/ubiquitination/proteasomal axis. These effects may contribute to the reduced renal concentrating ability that has been observed in dKO mice and underscore a physiologic mechanism of the CaSR-dependent regulation of AQP2 abundance *via* a novel microRNA pathway.—Ranieri, M., Zahedi, K., Tamma, G., Centrone, M., Di Mise, A., Soleimani, M., Valenti, G. CaSR signaling down-regulates AQP2 expression *via* a novel microRNA pathway in pendrin and NaCl cotransporter knockout mice. *FASEB J.* 32, 000–000 (2018). www.fasebj.org

KEY WORDS: water channel · miRNA-137 · p38-MAPK · hypercalciuria

The Cl⁻/HCO₃⁻ exchanger, pendrin (SLC26A4, PDS)—located on the apical membrane of β-intercalated cells in the kidney cortical collecting duct (CCD) and the connecting tubules (CNTs)—plays a dominant role in mediating the secretion of bicarbonate and the reabsorption of chloride (1–4), whereas, the thiazide-sensitive NaCl cotransporter (NCC) is primarily expressed on the apical membrane of distal convoluted tubule cells (5, 6) and represents the main sodium absorbing transporter in the distal convoluted tubule. The epithelial sodium channel is

the main molecule responsible for the absorption of sodium in CNTs and the CCD (5–13).

Chloride reabsorption in CNTs and the CCD is mediated *via* both paracellular and transcellular pathways, with the transcellular pathway being mediated primarily by pendrin, which, in conjunction with the epithelial sodium channel, is responsible for the bulk of sodium and chloride reabsorption in these two segments (14, 15).

Despite its critical role in the kidney, genetic deletion of pendrin does not cause any significant salt wasting or excessive diuresis in mutant mice under basal conditions, which suggests that this transporter does not play an important role in salt absorption under baseline conditions (16–18). Similar to pendrin-deficient mice, genetically engineered mice that lack NCC do not display excessive salt wasting under baseline conditions (12). Instead, NCC-deficient mice display enhanced calcium absorption along with magnesium wasting (12, 13). Of interest, whereas mice with a single deletion of NCC or pendrin have a mild

ABBREVIATIONS: AQP2, aquaporin-2; CaSR, calcium-sensing receptor; CCD, cortical collecting duct; CNT, connecting tubule; dKO, double knockout; GAPDH, glyceraldehyde-3-phosphate dehydrogenase; NCC, NaCl cotransporter; WT, wild type

¹ Correspondence: Department of Biosciences, Biotechnologies and Biopharmaceutics, University of Bari, Aldo Moro, Via Orabona 4, Amendola 165/A, 70125 Bari, Italy. E-mail: giovanna.valenti@uniba.it

doi: 10.1096/fj.201700412RR

phenotype, pendrin/NCC double-knockout (dKO) mice display significant salt wasting and develop severe volume depletion and metabolic alkalosis (19). These data indicate that pendrin and NCC cross-compensate for the loss of each other, masking the role that each transporter plays in salt reabsorption under baseline conditions (19).

One intriguing observation in pendrin/NCC dKO mice is the presence of hypercalciuria along with hyperphosphaturia (19). Consistently, calcium-absorbing pathway molecules—apical TRPV5 and basolateral Na⁺/Ca²⁺ exchanger—are down-regulated in KO mice (20).

The worsening of calcium reabsorption and the impaired reabsorption of sodium and phosphate have been proposed to be precipitated by severe salt wasting and volume depletion in dKO mice *via* processes mediated by prostaglandin E₂ (21).

Several lines of evidence demonstrate that hypercalciuria is associated with greater water excretion by the kidney. With respect to this, we have previously provided evidence that high concentrations of luminal calcium in the renal collecting duct counteract vasopressin action, thereby impairing the trafficking of the vasopressin-sensitive water channel, aquaporin 2 (AQP2). This effect is mediated by the activation of the calcium-sensing receptor (CaSR) (22, 23). Data that support this conclusion were obtained both from *in vitro* experiments using AQP2-expressing mouse collecting duct cells (MCD4 cells) and from hypercalciuric patients (24, 25), as well as from bed rest studies (25). Moreover, high external calcium has been found to reduce AQP2 expression, both in collecting duct cell lines and hypercalciuric rats (22, 26, 27). Specifically, CaSR activation in renal cells has been demonstrated to modulate AQP2 trafficking and/or expression by altering its phosphorylation state (28, 29), which indicates a direct negative effect on the vasopressin-sensitive water channel, AQP2. Of interest, pendrin/NCC dKO mice failed to increase their urine osmolality in response to desmopressin (dDAVP, a vasopressin analog), which is consistent with the impaired response to vasopressin, despite increased circulating levels of this hormone (19). Together, these data underscore a physiologic mechanism on the basis of negative feedback from CaSR signaling to AQP2 conferring high sensitivity of vasopressin to extracellular calcium (28, 30).

In the present work, we provide evidence that vasopressin resistance and possibly the volume depletion observed in pendrin/NCC dKO mice, in part, is a result of sustained CaSR signaling in the collecting duct, likely linked to high urinary calcium, that causes a bimodal down-regulation of AQP2 expression *via* the ubiquitin/degradative pathway and a novel microRNA pathway.

MATERIALS AND METHODS

Animal models

Double Slc26a4 pendrin/thiazide-sensitive NCC dKO mice were generated by crossing pendrin KO mice with NCC KO mice. Wild-type (WT) mice have a mixed BALB/c and C57BL/6J background (19).

Chemicals and reagents

All chemicals were purchased from Sigma-Aldrich (St. Louis, MO, USA). NPS-R568 was from Santa Cruz Biotechnology (Dallas, TX, USA) and NPS2143 from Tocris (Bristol, United Kingdom). SB203580 (p38-MAPK inhibitor) was from Cell Signaling Technology (Danvers, MA, USA). miRNA assay and kit were purchased from Applied Biosystems (Foster City, CA, USA).

Abs

AQP2 Abs against the 20-aa residue segment just N-terminal from the polyphosphorylated region of rat AQP2 (CLKGLEPDTDWEEREVRRRQ) (31, 32) were used to detect the total amount of AQP2. AQP2-pS261 Ab was from Novus Biologicals (Littleton, CO, USA). p38-MAPK, phospho-p38-MAPK (Thr180/Tyr182), and ubiquitin (P4D1) Abs were purchased from Cell Signaling Technology. mAb against glyceraldehyde-3-phosphate dehydrogenase (GAPDH; clone 6C5) was purchased from EMD Millipore (Billerica, MA, USA). Alexa Fluor 488 Abs were purchased from Thermo Fisher Scientific (Waltham, MA, USA).

Kidney slices from mouse inner medullary collecting ducts

Mouse kidney slices from mouse papilla were prepared as previously described (28, 33). In brief, WT and dKO mice—3 males and 2 females for each genotype—were anesthetized and euthanized by dislocation. Kidneys were quickly removed and ~500- μ m sections were made. Sectioned kidney papillae were equilibrated for 10 min in kidney slices buffer that contained 118 mM NaCl, 16 mM Hepes, 17 mM Na-Hepes, 14 mM glucose, 3.2 mM KCl, 2.5 mM CaCl₂, 1.8 mM MgSO₄, and 1.8 mM KH₂PO₄ (pH 7.4). Kidney slices were subsequently left in the same buffer at 37°C or incubated with 10 μ M NPS-R568 for 30 min or with 10 μ M NPS2143 for 30 min or desmopressin (dDAVP) 1 μ M for 30 min.

For experiments with p38-MAPK inhibitor, kidney slices were incubated with SB203580 at 10 μ M for 30 min. Treated sections were then homogenized with a mini-potter on ice-cold kidney slices buffer and protease and phosphatase inhibitors. Suspensions were then centrifuged at 12,000 g for 10 min at 4°C, and supernatants were used for Western blotting analysis.

Coimmunoprecipitation

Coimmunoprecipitation experiments were performed as previously described (34, 35). In brief, after treatments, kidney slices were lysed with 150 μ l of 1% Triton X-100, 150 mM NaCl, 25 mM Hepes (pH 7.4), and 20 mM N-ethylmaleimide to block deubiquitination in the presence of protease (1 mM PMSF, 2 mg/ml leupeptin, and 2 mg/ml pepstatin A) and phosphatase (10 mM NaF and 1 mM sodium orthovanadate) inhibitors. Lysates were clarified by centrifugation at 12,000 g for 20 min at 4°C. Supernatants obtained were precleared with protein A-sepharose suspension for 30 min under rotation at 4°C. Precleared lysates were incubated overnight at 4°C with anti-AQP2 Ab coupled to protein A-sepharose. Immunocomplexes were washed 3 times, resuspended in Laemmli's buffer in non-denaturing conditions, and subjected to immunoblotting using anti-AQP2 and anti-ubiquitin Abs.

Gel electrophoresis and Western blotting

Proteins were separated on 13% Bis-Tris acrylamide gels under reducing conditions. Protein bands were electrophoretically

transferred to immobilon-P membranes (EMD Millipore) for Western blot analysis, blocked in Tris-buffered saline—Tween-20 that contained 3% bovine serum albumin and incubated with primary Abs overnight. Immunoreactive bands were detected with secondary Ab conjugated to horseradish peroxidase obtained from Santa Cruz Biotechnology. Membranes were developed by using SuperSignal West Pico Chemiluminescent Substrate (Pierce, Rockford, IL, USA) with Chemidoc System (Bio-Rad, Hercules, CA, USA). Band intensities were quantified by densitometric analysis using Scion Image software (Scion, Frederick, MD, USA).

Immunolocalization in kidney tissue slices

For immunolocalization of AQP2 in mouse kidney slices (250 μm), tissues were incubated at 37°C for 15 min in kidney slices buffer only. After equilibration, slices were fixed by immersion in 4% paraformaldehyde in PBS at 4°C overnight. Slices were then rinsed several times in PBS before use for immunostaining. Sections were exposed to an antigen retrieval procedure with citrate buffer at pH 6 for 20 min. After washing in PBS, non-specific binding sites were then blocked with 1% bovine serum albumin in PBS (saturation buffer) overnight at 4°C. Sections were incubated with rabbit anti-AQP2 Ab (affinity purified; 1:3000 dilution) in saturation buffer overnight at 4°C. After washing in PBS, sections were incubated with secondary donkey anti-rabbit Alexa Fluor 488 conjugate (Thermo Fisher Scientific) for 2 h at room temperature. After washing in PBS, sections were mounted on glass slides with Mowiol (Sigma-Aldrich). Images were obtained with a confocal laser-scanning fluorescence microscope (TCS SP2; Leica Microsystems, Mannheim, Germany).

Real-time PCR analysis of mRNA of AQP2 and CaSR in WT and dKO mice

Real-time PCR experiments were performed to measure the relative expression of mRNA in inner medulla collecting duct (IMCD) that was isolated from WT and dKO mouse kidneys. Total RNA was extracted by using Trizol (Thermo Fisher Scientific). Reverse transcription was performed on 1 μg of total RNA using SuperScript Vilo Master Mix (Thermo Fisher Scientific). Real-time PCR amplification was performed by using TaqMan Gene Expression PCR Master Mix with AQP2 and GAPDH assays (Applied Biosystems) in StepOne Real-Time PCR System (Applied Biosystems). Results were expressed as $2^{-\Delta C_t}$ values (relative quantification) with $\Delta\Delta C_t = (C_{t\text{target}} - C_{t\text{GAPDH}})_{\text{dKO}} - (C_{t\text{target}} - C_{t\text{GAPDH}})_{\text{WT}}$.

miRNA-137 evaluation in WT and dKO mice

miRNA-137 content in WT and dKO mice inner medulla collecting duct was evaluated by using TaqMan Advanced miRNA Assays (has-miR-137; Assay ID: 477904_mir; Applied Biosystems), which enabled highly sensitive and specific quantification of mature miRNA using quantitative PCR. Total RNA was extracted by using Trizol. TaqMan Advanced miRNA cDNA Synthesis Kit (Applied Biosystems) was used to obtain cDNA synthesis. The synthetic RNA (UUAUUGCUUAAGAAUACGCGUAG) with 5'-phospho was synthesized by Applied Biosystems and used to perform a calibration line and interpolate miRNA sample values from WT and dKO mice to obtain the precise evaluation (ng) of miR137 content in samples.

Statistical analysis

One-way ANOVA followed by multiple comparison tests was used for statistical analysis. When applicable, a Student's *t* test

was also used, and for RT-PCR analysis, a 1-sample Student's *t* test was used. All values are expressed as means \pm SEM. Values of $P < 0.05$ were considered statistically significant.

RESULTS

Reduced expression of AQP2 in inner medulla of pendrin/NCC dKO mice

To evaluate AQP2 expression at the protein level, we performed immunoblotting experiments for AQP2 in inner medulla collecting duct samples from dKO and WT mice (Fig. 1A). Normalization of AQP2 immunoreactive bands to the housekeeping GAPDH revealed a strong (~65%) reduction in AQP2 levels in dKO mice compared with WT mice (dKO: 0.3597 ± 0.0666 OD *vs.* WT: 1.000 ± 0.2467 OD; $P < 0.05$; $n = 5$ for each genotype; Fig. 1A). In line with immunoblotting experiments, immunolocalization and analysis by confocal microscopy confirmed reduced expression of AQP2 in the inner medulla (Fig. 1B). Furthermore, evaluation of AQP2 mRNA that was extracted from the renal inner medulla collecting duct of WT and dKO mice and processed for real-time PCR revealed a strong reduction in mRNA in dKO mice compared with WT mice (dKO: 0.2869 ± 0.1031 *vs.* WT: 1.000; $*P < 0.001$, 1-sample Student's *t* test; $n = 8$ for each genotype; Fig. 1C). Conversely, no significant alteration at either the mRNA or protein levels was observed for AQP2 expressed in the cortex (data not shown).

Low AQP2 expression in the inner medulla of dKO mice is associated with significantly higher expression of AQP2-pS261 and phosphorylated p38-MAPK

AQP2 is subjected to a number of post-translational modifications, including phosphorylation and ubiquitination, that are important for AQP2 function and degradation (36, 37). Under vasopressin action, in the short term (within second to minutes), AQP2 is phosphorylated at S256, S269, S264, whereas, in the long term (within hours), AQP2 mRNA expression increases, followed by a rise in AQP2 protein level (38–40). Conversely, phosphorylation levels of Ser261 within the C terminus of AQP2 decreases in response to vasopressin (31, 38, 41, 42).

A role for AQP2 phosphorylation at Ser261 *via* p38-MAPK and polyubiquitination in the control of AQP2 protein degradation has been suggested (42, 43).

As the overall expression of AQP2 in the inner medulla of dKO mice is drastically reduced, we next evaluated whether this was in parallel to an increase in AQP2-pS261 levels. Levels of AQP2 phosphorylated at Ser261 (AQP2-pS261) were therefore semiquantified by Western blot experiments (Fig. 2A). Data obtained from these experiments demonstrated that AQP2-pS261 was significantly increased in dKO inner medulla compared with that of WT (normalized to total AQP2; dKO: 7.910 ± 0.7211 *vs.* WT: 1.000 ± 0.0588 ; $P < 0.0001$; $n = 5$ for each genotype; Fig. 2A). No significant alteration in AQP2-p256

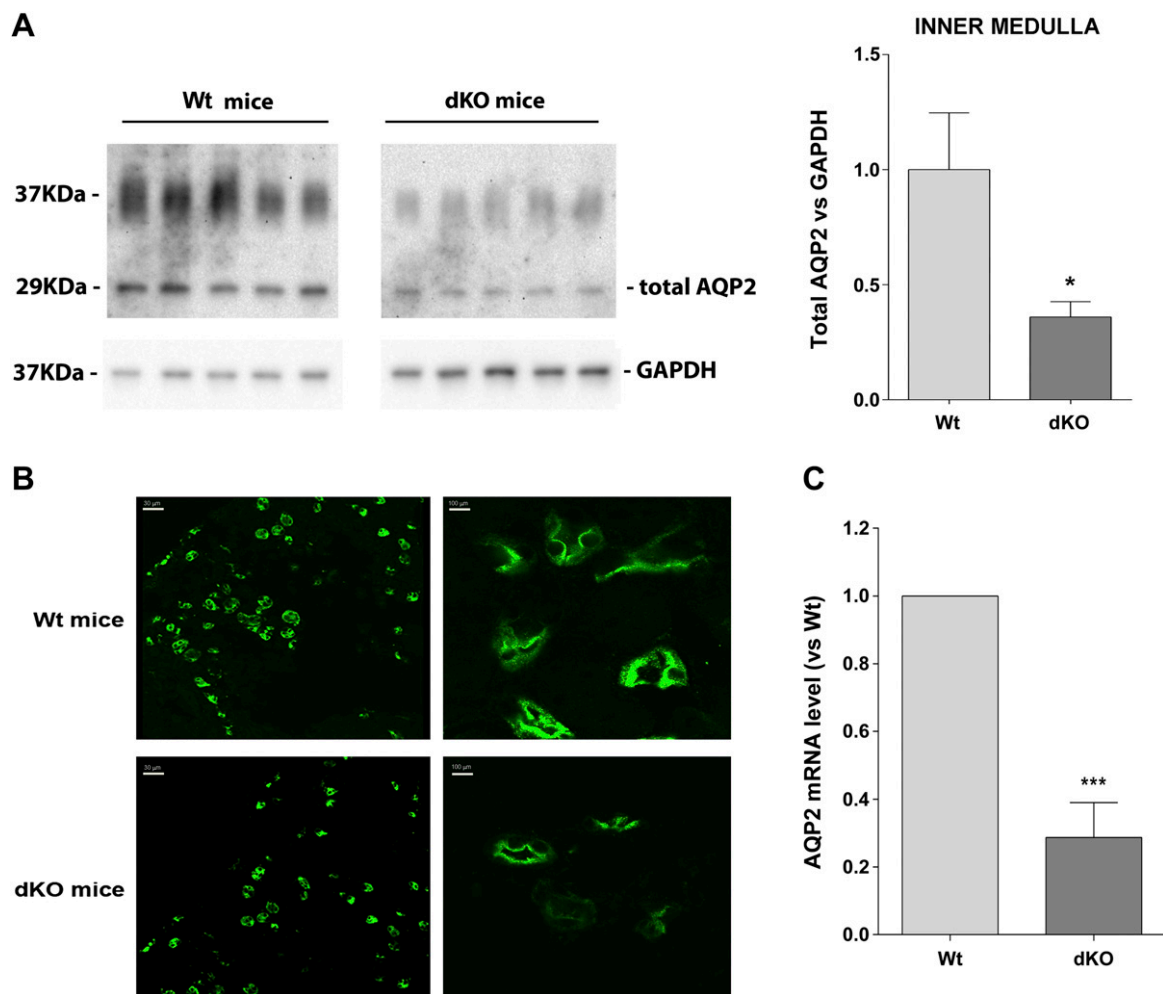


Figure 1. AQP2 expression and localization in the inner medulla collecting duct (IMCD) from WT and dKO mice. *A*) Inner medulla kidney slices from WT and dKO mice were lysed and subjected to immunoblotting using specific Abs against total AQP2. Protein content was normalized to the housekeeping protein, GAPDH. Signals from immunodetected bands were semiquantified by densitometry. AQP2 expression was significantly reduced in the inner medulla of dKO mice. $*P < 0.05$ vs. WT (Student's *t* test). *B*) Immunolocalization of AQP2 (in green) in the inner medulla of WT and dKO mice. Reduced AQP2 immunofluorescence signal was observed in dKO mice compared with WT mice. Scale bars: 30 μm (left), 100 μm (right). *C*) For analysis of AQP2 mRNA levels, RNA was extracted from WT and dKO mouse IMCD as described in Materials and Methods. RT-PCR experiments revealed that AQP2 mRNA levels were significantly reduced in dKO mice compared with WT mice. $***P < 0.001$ vs. WT (1-sample Student's *t* test). Data are presented as means \pm SEM.

level—normalized to total AQP2—was instead observed in dKO mice compared with WT mice ($n = 5$ for each genotype; data not shown).

p38-MAPK is a candidate kinase to phosphorylate AQP2 at Ser261 (31, 42) and is down-regulated by cAMP in a PKA-dependent manner; its phosphorylation represents a hallmark for ubiquitination and proteasomal degradation of AQP2 (42, 44). Phosphorylated p38-MAPK (Pp38-MAPK) represents the activated form of p38-MAPK and decreases upon vasopressin stimulation (42); therefore, we evaluated Pp38-MAPK levels using Western blot experiments (Fig. 2B). Statistical analysis of data revealed that Pp38-MAPK levels were ~ 2 -fold higher in dKO mice compared with WT mice (dKO: 1.822 ± 0.1616 vs. WT: 1.000 ± 0.088 ; $P < 0.01$; $n = 5$ for each genotype; Fig. 2B). These data point to p38-MAPK as a possible candidate kinase that is responsible for the increase in AQP2-pS261.

AQP2 in the inner medulla of dKO mice is more ubiquitinated and degraded via proteasome

Polyubiquitination targets proteins to proteasomes for degradation (45), and p38-MAPK activation results in proteasomal degradation of different proteins (46, 47). Of interest, evaluation of AQP2 expressed in the inner medulla of dKO mice demonstrated that, compared with WT mice, levels of ubiquitinated AQP2—both mono- and polyubiquitinated—normalized for immunoprecipitated AQP2 were ~ 4 -fold higher in the inner medulla of dKO mice (dKO: 3.892 ± 0.929 vs. WT: 1.000 ± 0.220 ; $P < 0.05$; $n = 3$ for each genotype; Fig. 3A).

AQP2 can be degraded in proteasomes and lysosomes (48, 49), and ubiquitination is a crucial step by which to direct proteins in both compartments (50). Therefore, we next assessed the effect of MG132 or chloroquine—inhibitors

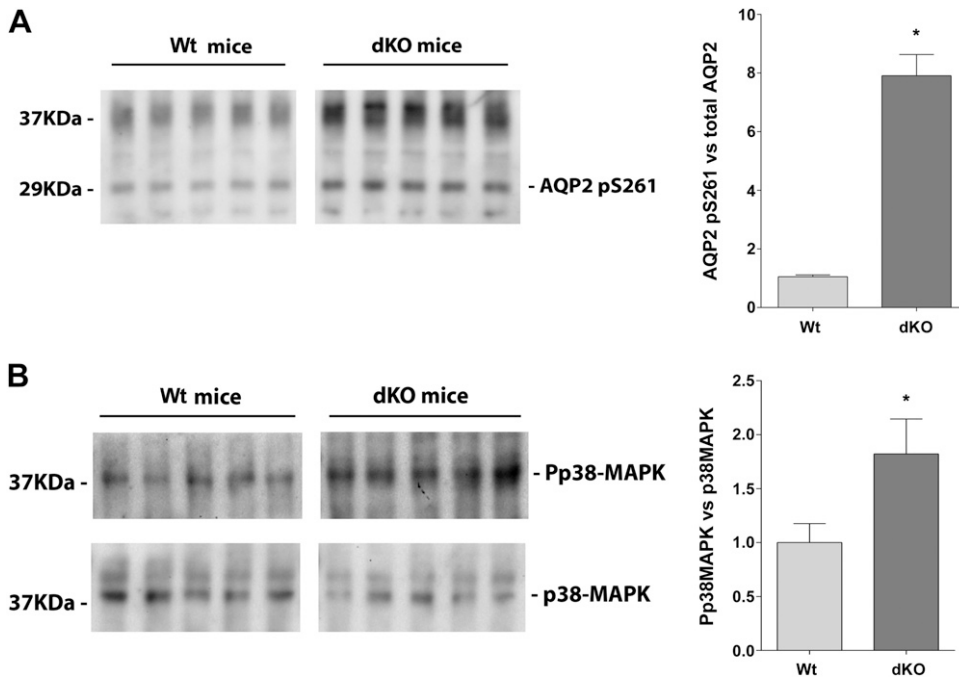


Figure 2. Phosphorylation of AQP2 at Ser261 and p38-MAPK in WT and dKO mice. Lysates from WT and dKO inner medulla kidney slices were subjected to immunoblotting using Abs against AQP2-pS261 and total AQP2 (A), or total p38-MAPK and its phosphorylated form, Pp38-MAPK (B). Statistical analysis of data revealed that in dKO mice, AQP2-pS261 normalized to total AQP2 was significantly increased. In parallel, a significant increase in Pp38-MAPK was observed in dKO mice. Data are presented as means \pm SEM. * $P < 0.05$ vs. WT.

of proteasomal and lysosomal degradation, respectively—on the expression of total AQP2 in inner medulla kidney slices ($n = 3$ for each genotype). Treatment of inner medulla kidney slices with chloroquine (100 μ M for 30 min) or MG132 (10 μ M for 30 min) in WT tissues had only a modest effect on total AQP2 abundance (Fig. 3B). In contrast in dKO kidney slices, while chloroquine had a slight effect ($\sim 15\%$ increase), MG132 was clearly more effective in increasing the total amount of AQP2 by nearly 50% (~ 5 -fold more effective than in WT; $P < 0.05$), which strongly suggested that the rate of AQP2 proteasomal degradation in dKO inner medulla is significantly higher than that in WT mice.

Role of CaSR signaling in the regulation of AQP2 abundance in dKO mice

We have recently demonstrated that the specific activation of CaSR expressed in the luminal membrane of the collecting duct prevents the cAMP-dependent increase in AQP2-pS256 and water permeability, which counteracts short-term vasopressin response (28, 30). We suggested that CaSR expressed in the collecting duct, as well as in the other segments of the nephron, exerts negative feedback on hormones that act *via* cAMP, which confers high sensitivity of hormone to extracellular calcium (30). Because dKO mice are extremely hypercalciuric, a tonic activation of CaSR in the collecting duct is expected in these mice, which, in turn, can modulate AQP2 trafficking and expression. First, a preliminary study confirmed that no significant differences, both at the mRNA and protein levels, were observed for CaSR expressed in the inner medulla between WT and dKO mice (data not shown).

To evaluate a direct link between CaSR signaling and the modulation of AQP2 expression, *ex vivo* experiments were performed by using dKO kidney slices from the inner medulla in the presence of NPS2143, a specific CaSR

allosteric inhibitor (51). Kidney slices from dKO mice were preincubated with 10 μ M NPS2143 for 30 min, and the effect on total AQP2 levels was assessed by Western blot analysis.

Of note, the sole exposure of dKO inner medulla kidney slices to the CaSR inhibitor, NPS2143 at rest, resulted in a strong increase (~ 3 -fold) in the level of total AQP2 (control: 1.000 ± 0.189 and NPS2143: 2.671 ± 0.173 ; $P < 0.05$; $n = 5$ for each treatment; Fig. 4A), which implies that CaSR signaling in dKO down-regulates AQP2 expression. Of interest, a similar effect on AQP2 down-regulation was obtained by exposing dKO inner medulla kidney slices to SB203580 (10 μ M for 30 min), a specific inhibitor of p38-MAPK (control: 1.000 ± 0.242 and SB203580: 5.097 ± 1.159 ; $P < 0.05$; $n = 3$ for each treatment; Fig. 4B), which indicates that this kinase is a downstream effector. Of note, preincubation of dKO kidney slices with NPS2143 also reduced AQP2-pS261 levels (control: 1.000 ± 0.031 and NPS2143: 0.497 ± 0.021 ; $P < 0.01$; $n = 3$ for each treatment; Fig. 4C). A comparable reduction in AQP2-pS261 levels was observed in the presence of SB203580 (control: 1.000 ± 0.153 , $P < 0.05$ and SB203580: 0.592 ± 0.055 ; $n = 3$ for each treatment; Fig. 4D), which suggests that CaSR signaling in dKO up-regulates AQP2-pS261 likely *via* p38-MAPK as a downstream effector in this pathway. The direct link between CaSR signaling and p38-MAPK activity was proven by demonstrating that preincubation of dKO kidney slices with NPS2143 also reduced Pp38-MAPK, the active form of p38-MAPK (control: 1.000 ± 0.111 and NPS2143: 0.546 ± 0.086 ; $P < 0.01$; $n = 5$ for each treatment; Fig. 4E). In line with this, SB203580 reduced Pp38-MAPK levels (control: 1.000 ± 0.184 and NPS2143: 0.144 ± 0.024 ; $P < 0.05$; $n = 5$ for each treatment; Fig. 4F). The final evidence that CaSR signaling in dKO modulates AQP2 expression by promoting AQP2 ubiquitination was obtained by exposing dKO inner medulla kidney slices to NPS2143 and SB203580, followed by

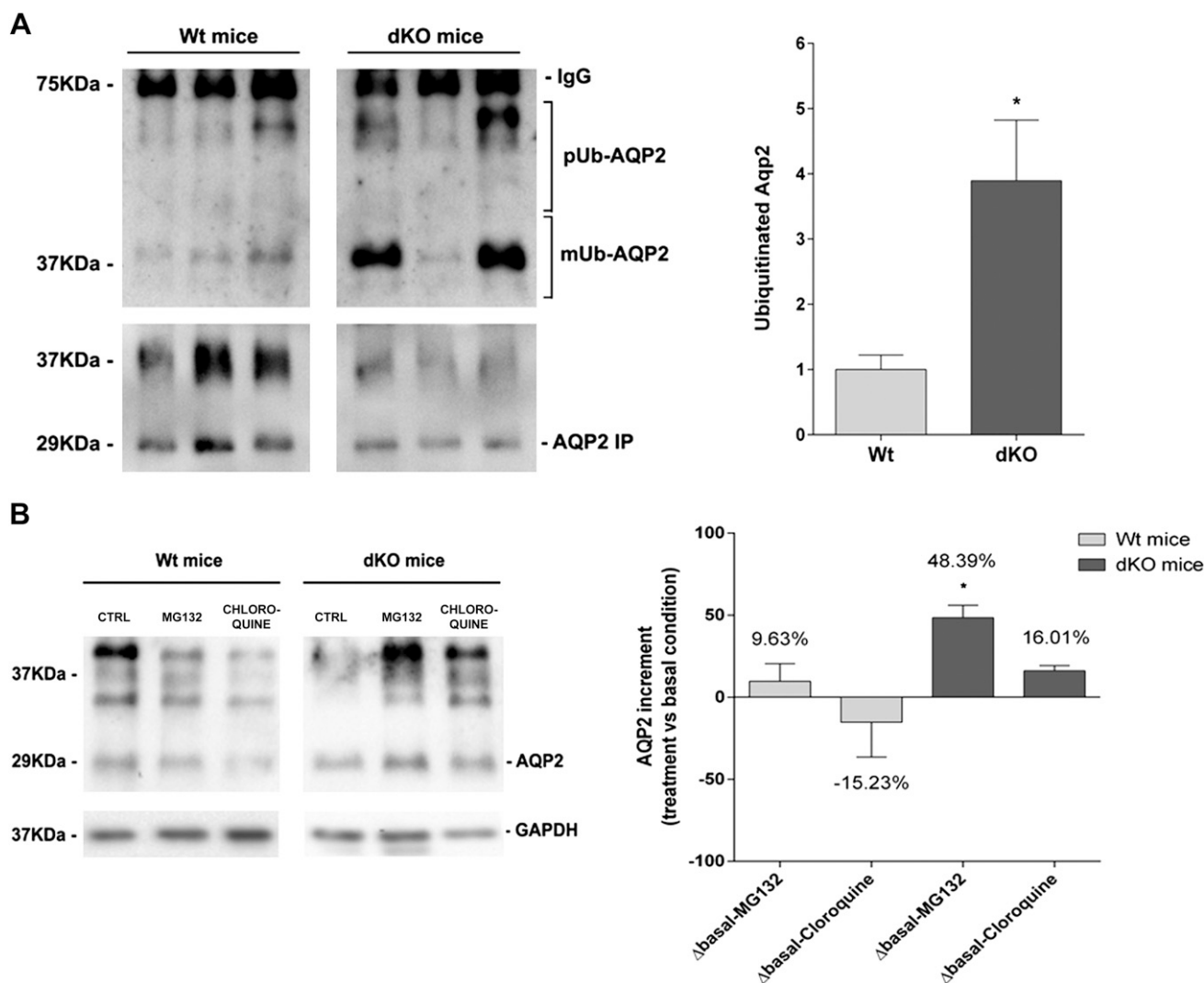


Figure 3. AQP2 ubiquitination and degradation in WT and dKO mice. *A*) Inner medulla kidney slices from WT and dKO mice were lysed and subjected to immunoprecipitation (IP) with AQP2 Ab. Immunoprecipitates were immunoblotted using anti-AQP2 and antiubiquitin Abs. Statistical analysis of data showed that ubiquitinated AQP2 (Ub-AQP2; both mono- and polyubiquitinated) levels normalized to immunoprecipitated AQP2 were significantly higher in the inner medulla of dKO mice. * $P < 0.05$ vs. WT. *B*) Inner medulla kidney slices from WT and dKO mice were lysated and immunoblotted using anti-AQP2 Ab and normalized to the housekeeping, GAPDH, to test the effect of proteasomal inhibitor, MG132, and the lysosomal inhibitor, chloroquine, on the expression of total AQP2. Rate of AQP2 proteasomal degradation in dKO inner medulla was significantly higher than that in WT mice. Data are presented as means \pm SEM percentage of difference between basal vs. MG132 and basal vs. chloroquine treatments.

semiquantitation of ubiquitinated AQP2. Both treatments resulted in a drastic decrease in ubiquitinated AQP2, which indicated that CaSR signaling in dKO plays a crucial role in decreasing total AQP2 levels, promoting AQP2 phosphorylation at Ser261 *via* the downstream effector, p38MAPK, which results in AQP2 ubiquitination (control: 1.000 ± 0.105 ; NPS2143: 0.274 ± 0.087 and SB203580: 0.360 ± 0.174 ; $P < 0.05$; $n = 3$ for each treatment; Fig. 4G).

CaSR signaling regulates AQP2 expression *via* microRNA pathway

The obtained data indicate that aberrant CaSR signaling in dKO mice can be responsible for the biased response of these mice to vasopressin (both at short and long term), whose levels are elevated in dKO mice (19), causing a

reduction of AQP2 expression as revealed by real-time PCR experiments (Fig. 1C).

On the basis of this idea, we investigated whether CaSR signaling in dKO mice regulates expression levels of miRNAs, which, in turn, transduce the extracellular signal *via* an miRNA-mediated reduction of AQP2 expression.

To this end, we evaluated miR-137, a known AQP2-targeting miRNA in the kidney collecting duct (52), in dKO mice. Of note, compared with WT mice, levels of miR137 observed in the kidney inner medulla of dKO mice were ~ 1.7 -fold higher (dKO: $2.867 \cdot 10^{-6} \pm 1.599 \cdot 10^{-7}$ ng vs. WT: $1.716 \cdot 10^{-6} \pm 8.704 \cdot 10^{-8}$ ng; $P < 0.0001$; $n = 7$ for each genotype; Fig. 5), leading to the intriguing hypothesis that regulation of miR-137 by CaSR signaling may be a crucial post-transcriptional modulator of AQP2 expression *via* inhibition of AQP2 mRNA translation.

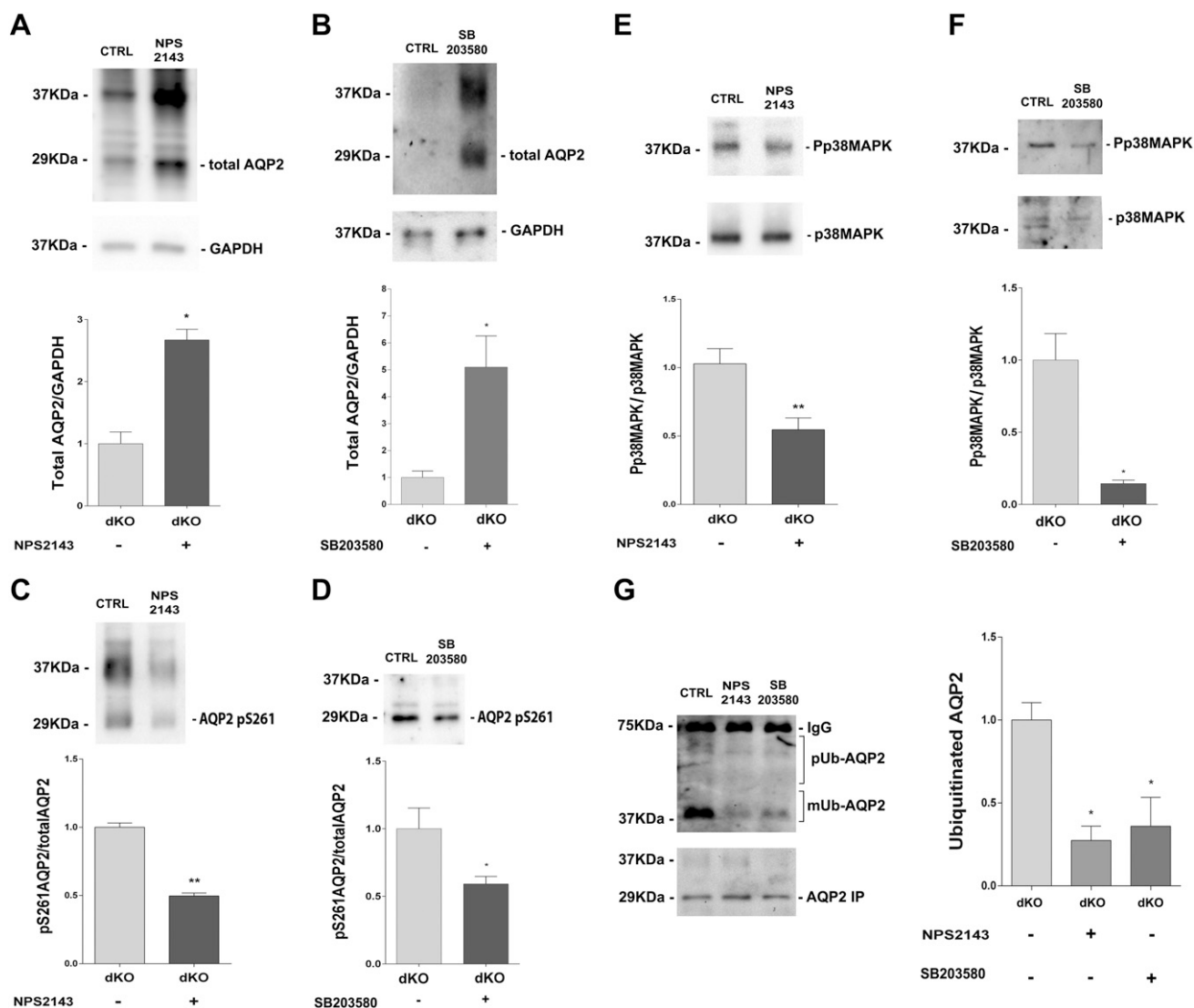


Figure 4. Effects of CaSR and p38-MAPK inhibition on total AQP2, AQP2-pS261, and ubiquitinated AQP2 (Ub-AQP2). Inner medulla kidney slices from WT and dKO mice were treated with the specific CaSR allosteric inhibitor, NPS2143 (A, C, E, G), or with the p38-MAPK inhibitor, SB203580 (B, D, F, G), lysed, and immunoblotted using specific Abs against total AQP2 or AQP2-pS261 or p38-MAPK and Pp38-MAPK. Statistical analysis of data revealed that, in dKO mice, the calcilytic NPS2143 caused an increase in total AQP2 (A) and a decrease in AQP2-pS261 (C) and a decrease in Pp38-MAPK (E). In dKO mice, p38-MAPK inhibitor increased total AQP2 levels (B), while decreased AQP2-pS261 (D) and Pp38-MAPK (F) levels. (G) Total lysates from dKO inner medulla kidney slices were treated with NPS2143 and SB203580, subjected to the immunoprecipitation, immunoblotted, and probed with AQP2 and ubiquitin Abs. Statistical analysis revealed that, in dKO mice, inhibition of CaSR and p38-MAPK significantly reduced ubiquitinated AQP2 levels. Data are presented as means \pm SEM. * $P < 0.05$ vs. dKO control (ctrl); ** $P < 0.01$ vs. dKO ctrl.

To evaluate this hypothesis, miR-137 levels were measured in the kidney inner medulla from WT and dKO mice under control conditions and after preincubation with NPS-R568 (10 μ M for 30 min) or NPS2143 (10 μ M for 30 min) to activate and inhibit CaSR, respectively (Fig. 6A, B). Quite interestingly, exposure of WT kidney slices to the CaSR allosteric activator, NPS-R568, resulted in a significant increase in miR-137 (control: 1.000 ± 0.102 and NPS-R568: 2.031 ± 0.328 ; $P < 0.01$; $n = 10$ for each treatment), which demonstrated a direct functional link between CaSR signaling and the production of AQP2-targeting miRNA (Fig. 6A). No significant effect on miR-137 levels was observed with treatment with the CaSR inhibitor, NPS2143 ($n = 10$ for each treatment), nor with SB203580

($n = 10$ for each treatment; Fig. 6A). In addition, no effect on miR-137 levels was observed after dDAVP stimulation (1 μ M for 30 min; control: 1.000 ± 0.102 and dDAVP: 0.972 ± 0.115 ; $n = 10$ for each treatment; data not shown), which was in agreement with previous findings that reported that miR-137 is not a vasopressin-regulated miRNA (52). Conversely, whereas exposure of dKO kidney slices to the CaSR allosteric activator, NPS-R568, had no effect on miR-137 (control: 1.000 ± 0.225 and NPS-R568: 0.723 ± 0.269 ; $n = 10$ for each treatment), a strong reduction in miR-137 level was obtained under treatment with the CaSR inhibitor, NPS2143 (control: 1.000 ± 0.225 and NPS2143: 0.215 ± 0.058 ; $P < 0.05$; $n = 10$ for each treatment), and with the p38 MAPK inhibitor, SB203580 (control: 1.000 ± 0.225

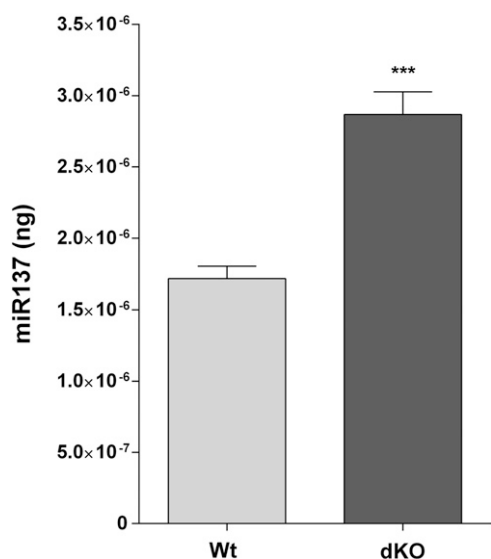


Figure 5. miR-137 evaluation in WT and dKO mice. Total RNA was extracted from WT and dKO mice inner medulla collecting duct, and the miRNA cDNA Synthesis Kit was used to obtain cDNA synthesis, as described in Materials and Methods. Synthetic RNA with 5'-phospho, miR-137 (UUAUUGC UUAAGAAUACGC-GUAG), was synthesized and used to perform a calibration line and interpolate miRNA sample values from WT and dKO mice to obtain a precise evaluation (in nanograms) of miR-137 content in samples. Data from RT-PCR experiments were interpolated in the calibration line obtained with synthetic miRNA. miR-137 levels were found to be significantly higher in dKO mice compared with WT mice. Data are presented as means \pm SEM. *** $P < 0.001$.

and SB203580: 0.266 ± 0.089 ; $P < 0.05$; $n = 10$ for each treatment).

Together, these data suggest that, at steady state, CaSR signaling reduces AQP2 expression also *via* miRNA pathway in dKO mice and that this pathway is mediated by p38-MAPK activation. Moreover, since the CaSR

inhibitor NPS2143 is effective only in the dKO inner medulla, this indicates that CaSR is constitutively more active in dKO mice, likely due to the tonic activation by high luminal calcium. Is particularly relevant that these data imply a physiologic role for CaSR expressed in the inner medulla in the modulation of total AQP2 expression *via* a novel miRNA pathway.

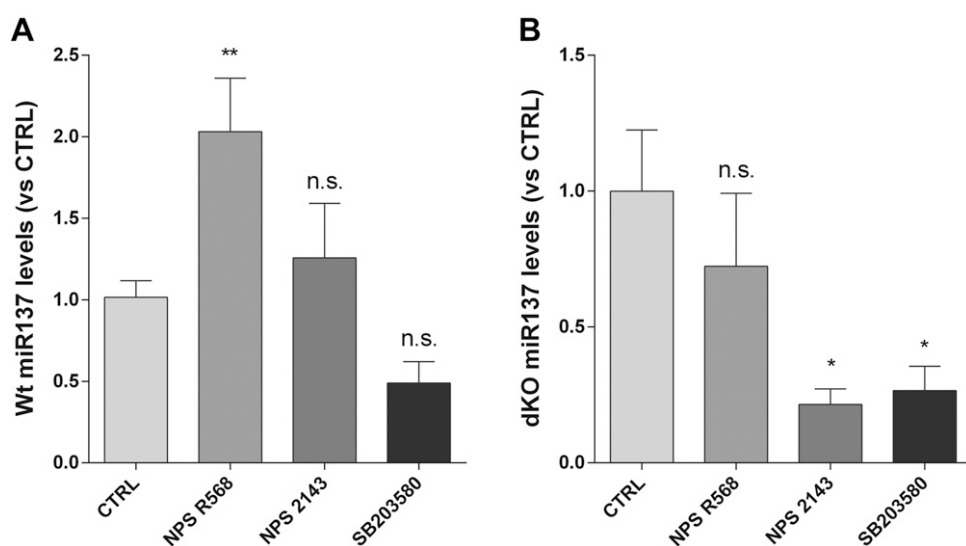
DISCUSSION

In the present study, we tested the hypothesis that vasopressin resistance and the consequent reduced renal concentrating ability in pendrin/NCC dKO mice is a result of a CaSR-mediated impairment of AQP2 expression/trafficking in the renal collecting duct.

Here, we have demonstrated that the activation of CaSR causes a bimodal down-regulation of AQP2 expression in dKO mice by increasing AQP2-pS261 levels *via* p38-MAPK, which results in enhanced AQP2 ubiquitination and degradation; and by a novel miRNA pathway, increasing miR-137, a known AQP2-targeting miRNA in the kidney collecting duct (52). The final effect of this CaSR signaling in dKO mice is to reduce collecting duct water permeability, which likely contributes to vasopressin resistance and possibly to the water depletion observed in dKO mice.

In the kidney, CaSR senses changes in both urine and serum calcium levels, which indicates a direct role in renal calcium handling (30). In the collecting duct, CaSR is expressed in intercalated cells and principal cells of the collecting duct (53) and is activated by luminal calcium. Specifically, in principal cells, CaSR is colocalized with the AQP2 water channel (30, 53, 54). Several *in vitro* and *in vivo* studies, including those in humans, have suggested that CaSR signaling inhibits vasopressin-induced trafficking and expression of AQP2 (22, 24–26, 28, 55–58). The proposed mechanism for this process is that vasopressin-regulated water reabsorption from the lumen causes an

Figure 6. Modulation of miR-137 in response to CaSR activation or CaSR and p38-MAPK inhibition in WT and dKO mice. Total RNA was extracted from WT and dKO mice inner medulla collecting duct under different experimental conditions, and the miRNA cDNA Synthesis Kit was used to obtain cDNA synthesis. *A*) In WT mice, CaSR activation with NPS-R568 (10 μ M for 30 min) caused a significant increase in miR-137 compared with control (ctrl). No significant change in miR-137 levels was observed after treatment with the calcilytic NPS2143 (10 μ M for 30 min) or the SB203580 p38-MAPK inhibitor (10 μ M for 30 min). ** $P < 0.01$ vs. ctrl. *B*) In dKO mice, CaSR activation with NPS-R568 (10 μ M for 30 min) did not alter miR-137 levels compared with control, whereas treatment with the calcilytic NPS2143 (10 μ M for 30 min) or the SB203580 p38-MAPK inhibitor (10 μ M for 30 min) caused a drastic decrease in miR-137 levels compared with control. * $P < 0.05$ vs. ctrl. N.s., not significant. Data are presented as means \pm SEM.



increase in urinary calcium levels as a result of urine concentration, which, in turn, activates CaSR located on the apical membrane of the principal cells. Activation of CaSR reduces the vasopressin-stimulated insertion of AQP2 into the plasma membrane and the rate of water reabsorption, which leads to the formation of dilute urine and, consequently, a reduced risk of calcium supersaturation (22–24, 28). Whereas the acute inhibitory effect of CaSR signaling on vasopressin-activated AQP2 trafficking and water reabsorption is mainly due to a strong reduction in cAMP-induced AQP2 phosphorylation at Ser256 (28), the sustained activation of CaSR—as mimicked by the ectopic expression of CaSR gain-of-function variants (hCaSR-R990G, hCaSR-N124K)—was found to cause a significant increase in AQP2-pS261 levels (28). In line with this, in pendrin/NCC dKO mice, which display severe hypercalciuria, a tonic activation of the luminal CaSR in the collecting duct is expected and was found here to be associated with a strong reduction in total AQP2 expression. Nevertheless, when normalized to total AQP2, a significantly higher expression of AQP2-pS261 was observed, along with higher levels of ubiquitinated AQP2. In addition, in dKO mice, sensitivity to the proteasome inhibitor, MG132, was found to be 5-fold higher than in WT mice, as exposure of inner medulla kidney slices to MG132 increased total AQP2 by >50% (Fig. 3). Overall, these data indicate that, in the dKO inner medulla, the rate of AQP2 degradation *via* proteasome is significantly higher than that in WT mice. It should be noted that the experiments were conducted using the tip of the inner medulla collecting duct from dKO mice, thereby excluding the contribution of CaSR expressed in the thick ascending limb, where the highest expression of CaSR is found.

Several authors have suggested a critical role for AQP2 phosphorylation at Ser261 and polyubiquitination in the control of AQP2 levels (42, 43). Specifically, a role for p38-MAPK in the promotion of AQP2 phosphorylation at Ser261 has been reported (42, 43).

Here, we report that, in dKO inner medulla kidney slices, p38-MAPK expression was found to be ~2.5-fold higher compared with that of WT. Moreover, SB203580, a specific inhibitor of p38-MAPK, caused a drastic decrease in p38-MAPK phosphorylation—the active form of MAPK—and in AQP2-pS261, along with a nearly 5-fold increase in total AQP2 (Fig. 4). In addition, SB203580 drastically reduced the levels of ubiquitinated AQP2 (Fig. 4), which indicates that p38-MAPK is the kinase committed to phosphorylate AQP2 at Ser261, likely promoting AQP2 ubiquitination. Polyubiquitination targets proteins to proteasomes (45), and p38-MAPK activation results in proteasomal degradation of different proteins (46, 47). Consistent with these findings, we demonstrate here that, in dKO, p38-MAPK inhibition results in a drastic reduction in ubiquitinated AQP2 that is paralleled by a strong increase in total AQP2 (Fig. 4).

Previous work has demonstrated that p38-MAPK is a downstream effector of CaSR. Specifically, CaSR activation associated with high extracellular calcium causes the rapid and highly significant p38-MAPK phosphorylation in a kidney proximal epithelial cell model, in airway

smooth muscle cells, and in H-500 Leydig cancer cells (59–61), which indicates that CaSR activation induces p38-MAPK phosphorylation.

Data presented here directly demonstrate that, in dKO mice, CaSR signaling *via* p38-MAPK is the key to the mechanism of reduced AQP2 abundance. In fact, the CaSR inhibitor, NPS2143, caused a strong reduction in Pp38-MAPK, reproducing the same effects observed in response to specific p38-MAPK inhibition—that is, increased total AQP2 abundance and reduced AQP2-pS261 and ubiquitinated AQP2 levels, which point to CaSR as the upstream receptor that orchestrates the modulation of AQP2 expression (Fig. 4).

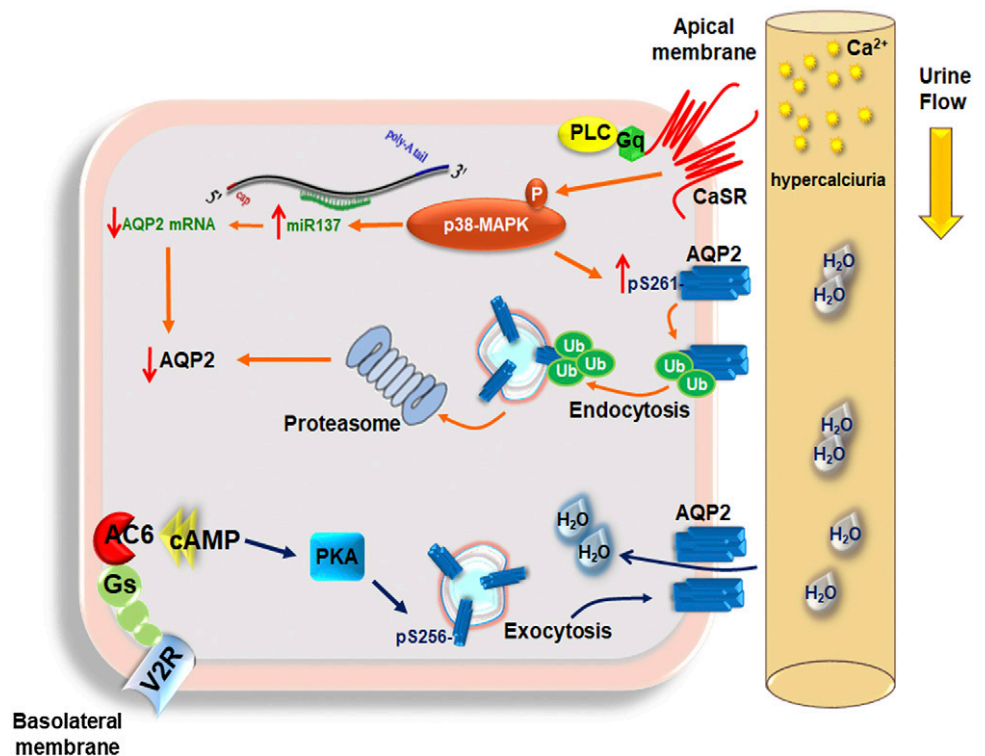
Our data suggest that, in addition to the enhanced rate of AQP2 degradation, low AQP2 levels observed in dKO mice are also a result of reduced AQP2 mRNA translation *via* a novel miRNA pathway that is modulated by CaSR signaling. miRNAs are single-stranded, noncoding RNA molecules ~21 nt (62), and base paired with their target mRNAs, inducing mRNA translational repression (55).

In the kidney inner medulla of dKO mice, miR-137, a known AQP2-targeting miRNA in the renal collecting duct (52), was found to be ~1.7-fold higher compared to WT mice, which was in line with the reduced translation of AQP2 mRNA. Worthy of attention, under physiologic conditions in WT mice, miR-137 transcript levels were increased by the calcimimetic NPS-R568 (Fig. 6), providing the first evidence that CaSR signaling directly acts upstream of the miR-137–AQP2 axis. Conversely, whereas in dKO mice, exposure to NPS-R568 had no effect on miR-137 levels (likely because of the tonic CaSR activation by high luminal calcium), compared with WT, a strong reduction in miR-137 levels was observed under treatment with the CaSR inhibitor, NPS2143, as well as with the p38-MAPK inhibitor, providing direct evidence that CaSR can regulate AQP2 expression *via* AQP2-targeting miRNA in a pathophysiological setting.

In a previous study (56), CaSR signaling was shown to modulate gene expression *via* miRNA in the kidney thick ascending limb of Henle. Hou and coworkers (56) demonstrated that in the thick ascending limb, high external calcium—*via* activation of CaSR—regulates the expression levels of 2 miRNAs, miR-9 and miR-374, which, in turn, reduces the expression of Claudin-14, a protein that blocks the paracellular cation channel, leading to decreases in cation permeation. These data indicate that the regulation of miRNA by CaSR signaling may occur on several layers within the kidney.

Despite several studies that have demonstrated that transcriptional and post-transcriptional regulation of AQP2 play a crucial role in AQP2 expression levels within the cell, along with a profound impact on water homeostasis (36, 57), little is known about the role of miRNA in the regulation of AQP2 expression. In this respect, the report by Kwon and coworkers (52) demonstrated that a significant decrease of AQP2 translation is observed in mpkCCDC14 cells when these cells were transfected with miR-32 or miR-137. In addition, the authors demonstrated that both miR-32 and miR-137 are AQP2-targeting miRNAs in kidney collecting duct cells and result in the vasopressin-independent regulation of AQP2. In line with

Figure 7. Schematic model. The proposed model shows that, in dKO mice, higher urinary calcium levels activate CaSR, resulting in the activation and phosphorylation of p38-MAPK that, in turn, phosphorylates AQP2 at Ser261, causing AQP2 internalization, ubiquitination (Ub), and proteasomal degradation. In parallel, CaSR signaling promotes the synthesis of miRNA-137 *via* the activation of p38-MAPK, which results in reduced AQP2 mRNA translation. For more details, see Discussion.



these findings, in the pathophysiological setting of the pendrin/NCC dKO mice analyzed here, we show significantly higher miR-137 transcript levels compared with the WT strain, which are drastically reduced in response to CaSR or p38-MAPK inhibition. Moreover, in WT mice, CaSR activation with calcimimetics, and not with dDAVP (data not shown), caused a significant increase in miR-137, providing the first novel evidence that CaSR signaling directly regulates, in part, AQP2 protein expression *via* RNA interference—AQP2-targeting miRNAs—in a vasopressin-independent manner.

It should be noted that other pathways, such as the high urinary prostaglandin E₂ levels in pendrin/NCC dKO mice (21), can also contribute to the reduced AQP2 expression, as previously reported (58, 63). Increase in prostaglandin E₂ in dKO mice was paralleled with an increase in cyclooxygenase-2 (21), and it is known that CaSR induces cyclooxygenase-2, which leads to the synthesis of prostaglandin E₂ (64, 65). Therefore, although we do not provide direct *in vivo* data that CaSR activation contributes to vasopressin resistance and polyuria in dKO mice, indirect *in vivo* and direct *ex vivo* data strongly support this hypothesis. In line with this, recent data indicate that hypercalcemia-induced hypercalciuria, by exposing cells to sustained elevated extracellular calcium, causes AQP2 autophagic degradation that is mediated by CaSR activation (66). Cell-surface AQP2 abundance is crucial to the maintenance of body water homeostasis; however, it should be considered that dKO mice may also have a moderate defect in the generation of the cortical-medullary gradient as a result of the down-regulation of NKCC2 (20), which is also critical for the production of concentrated urine. Therefore, both aspects have account for to explain the polyuria and volume depletion in dKO mice.

In summary, we propose that, in pendrin/NCC dKO mice, a bimodal down-regulation of AQP2 expression occurs: *i)* *via* p38-MAPK-dependent increased AQP2-pS261 and AQP2 ubiquitination leading to AQP2 protein degradation, and *ii)* *via* the AQP2-targeting miR-137 pathway. Both pathways have been demonstrated to be directly activated by CaSR signaling and to contribute to vasopressin resistance and the consequent reduced renal concentrating ability in pendrin/NCC dKO mice (proposed model in Fig. 7). Notably, our data on a mouse-based genetic model unravel the molecular basis of a novel physiological mechanism that, in the renal inner medulla, may link the activation of CaSR to the regulation of the expression levels of miRNAs regulating AQP2 expression. [F]

ACKNOWLEDGMENTS

The authors thank Elena Ciani (University of Bari) for assistance with real-time PCR experiments. M.R. is a post-doctoral research fellow supported by “Intervento cofinanziato dal Fondo di Sviluppo e Coesione 2007-2013-APQ Ricerca Regione Puglia Programma Regionale a Sostegno della Specializzazione Intelligente e della Sostenibilità Sociale ed Ambientale-FutureInResearch.” This study was supported, in part, by Telethon funding (GGP13227) and by Italian Space Agency (ASI; 2013-091-R.0 to G.V.), by Progetti di Rilevante Interesse Nazionale (PRIN; 01373409 to G.T.), and by Merit Review Award 2IO1BX001000 (Grant 12111018 to M.S.). The authors declare no conflicts of interest.

AUTHOR CONTRIBUTIONS

M. Ranieri, M. Soleimani, and G. Valenti designed research and supervised the project; M. Ranieri, K. Zahedi, M. Centrone, and A. Di Mise performed research

and analyzed data; M. Ranieri, G. Tamma, and G. Valenti designed and interpreted experiments; M. Ranieri and G. Valenti wrote the paper; and all authors commented on the manuscript.

REFERENCES

- Kim, Y. H., Kwon, T. H., Frische, S., Kim, J., Tisher, C. C., Madsen, K. M., and Nielsen, S. (2002) Immunocytochemical localization of pendrin in intercalated cell subtypes in rat and mouse kidney. *Am. J. Physiol. Renal Physiol.* **283**, F744–F754
- Wall, S. M., Hassell, K. A., Royaux, I. E., Green, E. D., Chang, J. Y., Shipley, G. L., and Verlander, J. W. (2003) Localization of pendrin in mouse kidney. *Am. J. Physiol. Renal Physiol.* **284**, F229–F241
- Petrovic, S., Wang, Z., Ma, L., and Soleimani, M. (2003) Regulation of the apical Cl⁻/HCO₃⁻ exchanger pendrin in rat cortical collecting duct in metabolic acidosis. *Am. J. Physiol. Renal Physiol.* **284**, F103–F112
- Tamma, G., Ranieri, M., Dossena, S., Di Mise, A., Nofziger, C., Svelto, M., Paulmichl, M., and Valenti, G. (2013) A FRET-based approach for quantitative evaluation of forskolin-induced pendrin trafficking at the plasma membrane in bronchial NCI H292 cells. *Cell. Physiol. Biochem.* **32**, 200–209
- Câmpean, V., Kricke, J., Ellison, D., Luft, F. C., and Bachmann, S. (2001) Localization of thiazide-sensitive Na⁺-Cl⁻ cotransport and associated gene products in mouse DCT. *Am. J. Physiol. Renal Physiol.* **281**, F1028–F1035
- Delpire, E., and Mount, D. B. (2002) Human and murine phenotypes associated with defects in cation-chloride cotransport. *Annu. Rev. Physiol.* **64**, 803–843
- Gamba, G. (2005) Molecular physiology and pathophysiology of electroneutral cation-chloride cotransporters. *Physiol. Rev.* **85**, 423–493
- Ellison, D. H. (2003) The thiazide-sensitive Na-Cl cotransporter and human disease: reemergence of an old player. *J. Am. Soc. Nephrol.* **14**, 538–540
- Delpire, E., Kaplan, M. R., Plotkin, M. D., and Hebert, S. C. (1996) The Na-(K)-Cl cotransporter family in the mammalian kidney: molecular identification and function(s). *Nephrol. Dial. Transplant.* **11**, 1967–1973
- Ellison, D. H., Velázquez, H., and Wright, F. S. (1989) Adaptation of the distal convoluted tubule of the rat. Structural and functional effects of dietary salt intake and chronic diuretic infusion. *J. Clin. Invest.* **83**, 113–126
- Ellison, D. H., Velázquez, H., and Wright, F. S. (1987) Thiazide-sensitive sodium chloride cotransport in early distal tubule. *Am. J. Physiol.* **253**, F546–F554
- Schultheis, P. J., Lorenz, J. N., Meneton, P., Nieman, M. L., Riddle, T. M., Flagella, M., Duffy, J. J., Doetschman, T., Miller, M. L., and Shull, G. E. (1998) Phenotype resembling Gitelman's syndrome in mice lacking the apical Na⁺-Cl⁻ cotransporter of the distal convoluted tubule. *J. Biol. Chem.* **273**, 29150–29155
- Loffing, J., Vallon, V., Loffing-Cueni, D., Aregger, F., Richter, K., Pietri, L., Bloch-Faure, M., Hoenderop, J. G., Shull, G. E., Meneton, P., and Kaissling, B. (2004) Altered renal distal tubule structure and renal Na⁺ and Ca²⁺ handling in a mouse model for Gitelman's syndrome. *J. Am. Soc. Nephrol.* **15**, 2276–2288
- Wall, S. M., and Pech, V. (2008) The interaction of pendrin and the epithelial sodium channel in blood pressure regulation. *Curr. Opin. Nephrol. Hypertens.* **17**, 18–24
- Wall, S. M., and Weinstein, A. M. (2013) Cortical distal nephron Cl⁻ transport in volume homeostasis and blood pressure regulation. *Am. J. Physiol. Renal Physiol.* **305**, F427–F438
- Royaux, I. E., Wall, S. M., Karniski, L. P., Everett, L. A., Suzuki, K., Knepper, M. A., and Green, E. D. (2001) Pendrin, encoded by the Pendred syndrome gene, resides in the apical region of renal intercalated cells and mediates bicarbonate secretion. *Proc. Natl. Acad. Sci. USA* **98**, 4221–4226
- Verlander, J. W., Hassell, K. A., Royaux, I. E., Glapion, D. M., Wang, M. E., Everett, L. A., Green, E. D., and Wall, S. M. (2003) Deoxycorticosterone upregulates PDS (Slc26a4) in mouse kidney: role of pendrin in mineralocorticoid-induced hypertension. *Hypertension* **42**, 356–362
- Amlal, H., Petrovic, S., Xu, J., Wang, Z., Sun, X., Barone, S., and Soleimani, M. (2010) Deletion of the anion exchanger Slc26a4 (pendrin) decreases apical Cl⁻/HCO₃⁻ exchanger activity and impairs bicarbonate secretion in kidney collecting duct. *Am. J. Physiol. Cell Physiol.* **299**, C33–C41
- Soleimani, M., Barone, S., Xu, J., Shull, G. E., Siddiqui, F., Zahedi, K., and Amlal, H. (2012) Double knockout of pendrin and Na-Cl cotransporter (NCC) causes severe salt wasting, volume depletion, and renal failure. *Proc. Natl. Acad. Sci. USA* **109**, 13368–13373
- Gkika, D., Hsu, Y. J., van der Kemp, A. W., Christakos, S., Bindels, R. J., and Hoenderop, J. G. (2006) Critical role of the epithelial Ca²⁺ channel TRPV5 in active Ca²⁺ reabsorption as revealed by TRPV5/calbindin-D28K knockout mice. *J. Am. Soc. Nephrol.* **17**, 3020–3027
- Soleimani, M., Barone, S., Xu, J., Alshahrani, S., Brooks, M., McCormack, F. X., Smith, R. D., and Zahedi, K. (2016) Prostaglandin-E₂ mediated increase in calcium and phosphate excretion in a mouse model of distal nephron salt wasting. *PLoS One* **11**, e0159804
- Procino, G., Carosino, M., Tamma, G., Gouraud, S., Laera, A., Riccardi, D., Svelto, M., and Valenti, G. (2004) Extracellular calcium antagonizes forskolin-induced aquaporin 2 trafficking in collecting duct cells. *Kidney Int.* **66**, 2245–2255
- Procino, G., Mastrofrancesco, L., Mira, A., Tamma, G., Carosino, M., Emma, F., Svelto, M., and Valenti, G. (2008) Aquaporin 2 and apical calcium-sensing receptor: new players in polyuric disorders associated with hypercalciuria. *Semin. Nephrol.* **28**, 297–305
- Procino, G., Mastrofrancesco, L., Tamma, G., Lasorsa, D. R., Ranieri, M., Stringini, G., Emma, F., Svelto, M., and Valenti, G. (2012) Calcium-sensing receptor and aquaporin 2 interplay in hypercalciuria-associated renal concentrating defect in humans. An *in vivo* and *in vitro* study. *PLoS One* **7**, e33145
- Tamma, G., Di Mise, A., Ranieri, M., Svelto, M., Pisot, R., Bilancio, G., Cavallo, P., De Santo, N. G., Cirillo, M., and Valenti, G. (2014) A decrease in aquaporin 2 excretion is associated with bed rest induced high calciuria. *J. Transl. Med.* **12**, 133
- Bustamante, M., Hasler, U., Leroy, V., de Seigneux, S., Dimitrov, M., Mordasini, D., Rousselot, M., Martin, P. Y., and Féraille, E. (2008) Calcium-sensing receptor attenuates AVP-induced aquaporin-2 expression *via* a calmodulin-dependent mechanism. *J. Am. Soc. Nephrol.* **19**, 109–116
- Sands, J. M., Flores, F. X., Kato, A., Baum, M. A., Brown, E. M., Ward, D. T., Hebert, S. C., and Harris, H. W. (1998) Vasopressin-elicited water and urea permeabilities are altered in IMCD in hypercalcemic rats. *Am. J. Physiol.* **274**, F978–F985
- Ranieri, M., Tamma, G., Di Mise, A., Russo, A., Centrone, M., Svelto, M., Calamita, G., and Valenti, G. (2015) Negative feedback from CaSR signaling to aquaporin-2 sensitizes vasopressin to extracellular Ca²⁺. *J. Cell Sci.* **128**, 2350–2360
- Ranieri, M., Tamma, G., Di Mise, A., Vezzoli, G., Soldati, L., Svelto, M., and Valenti, G. (2013) Excessive signal transduction of gain-of-function variants of the calcium-sensing receptor (CaSR) are associated with increased ER to cytosol calcium gradient. *PLoS One* **8**, e79113
- Riccardi, D., and Valenti, G. (2016) Localization and function of the renal calcium-sensing receptor. *Nat. Rev. Nephrol.* **12**, 414–425
- Hoffert, J. D., Pisitkun, T., Wang, G., Shen, R. F., and Knepper, M. A. (2006) Quantitative phosphoproteomics of vasopressin-sensitive renal cells: regulation of aquaporin-2 phosphorylation at two sites. *Proc. Natl. Acad. Sci. USA* **103**, 7159–7164
- Tamma, G., Lasorsa, D., Ranieri, M., Mastrofrancesco, L., Valenti, G., and Svelto, M. (2011) Integrin signaling modulates AQP2 trafficking *via* Arg-Gly-Asp (RGD) motif. *Cell. Physiol. Biochem.* **27**, 739–748
- Boone, M., Kortenoeven, M. L., Robben, J. H., Tamma, G., and Deen, P. M. (2011) Counteracting vasopressin-mediated water reabsorption by ATP, dopamine, and phorbol esters: mechanisms of action. *Am. J. Physiol. Renal Physiol.* **300**, F761–F771
- Valenti, G., Mira, A., Mastrofrancesco, L., Lasorsa, D. R., Ranieri, M., and Svelto, M. (2010) Differential modulation of intracellular Ca²⁺ responses associated with calcium-sensing receptor activation in renal collecting duct cells. *Cell. Physiol. Biochem.* **26**, 901–912
- Di Mise, A., Tamma, G., Ranieri, M., Svelto, M., Heuvel, B., Levchenko, E. N., and Valenti, G. (2015) Conditionally immortalized human proximal tubular epithelial cells isolated from the urine of a healthy subject express functional calcium-sensing receptor. *Am. J. Physiol. Renal Physiol.* **308**, F1200–F1206
- Moeller, H. B., Olesen, E. T., and Fenton, R. A. (2011) Regulation of the water channel aquaporin-2 by posttranslational modification. *Am. J. Physiol. Renal Physiol.* **300**, F1062–F1073
- Tamma, G., Ranieri, M., Di Mise, A., Centrone, M., Svelto, M., and Valenti, G. (2014) Glutathionylation of the aquaporin-2 water

- channel: a novel post-translational modification modulated by the oxidative stress. *J. Biol. Chem.* **289**, 27807–27813
38. Matsumura, Y., Uchida, S., Rai, T., Sasaki, S., and Marumo, F. (1997) Transcriptional regulation of aquaporin-2 water channel gene by cAMP. *J. Am. Soc. Nephrol.* **8**, 861–867
 39. Fenton, R. A., and Moeller, H. B. (2008) Recent discoveries in vasopressin-regulated aquaporin-2 trafficking. *Prog. Brain Res.* **170**, 571–579
 40. Hoffert, J. D., Fenton, R. A., Moeller, H. B., Simons, B., Tchapyjnikov, D., McDill, B. W., Yu, M. J., Pisitkun, T., Chen, F., and Knepper, M. A. (2008) Vasopressin-stimulated increase in phosphorylation at Ser269 potentiates plasma membrane retention of aquaporin-2. *J. Biol. Chem.* **283**, 24617–24627
 41. Hoffert, J. D., Nielsen, J., Yu, M. J., Pisitkun, T., Schleicher, S. M., Nielsen, S., and Knepper, M. A. (2007) Dynamics of aquaporin-2 serine-261 phosphorylation in response to short-term vasopressin treatment in collecting duct. *Am. J. Physiol. Renal Physiol.* **292**, F691–F700
 42. Nedvetsky, P. I., Tabor, V., Tamma, G., Beulshausen, S., Skroblin, P., Kirschner, A., Mutig, K., Boltzen, M., Petrucci, O., Vossenkämper, A., Wiesner, B., Bachmann, S., Rosenthal, W., and Klusmann, E. (2010) Reciprocal regulation of aquaporin-2 abundance and degradation by protein kinase A and p38-MAP kinase. *J. Am. Soc. Nephrol.* **21**, 1645–1656
 43. Trepiccione, F., Pisitkun, T., Hoffert, J. D., Poulsen, S. B., Capasso, G., Nielsen, S., Knepper, M. A., Fenton, R. A., and Christensen, B. M. (2014) Early targets of lithium in rat kidney inner medullary collecting duct include p38 and ERK1/2. *Kidney Int.* **86**, 757–767
 44. Isobe, K., Jung, H. J., Yang, C. R., Claxton, J., Sandoval, P., Burg, M. B., Raghuram, V., and Knepper, M. A. (2017) Systems-level identification of PKA-dependent signaling in epithelial cells. *Proc. Natl. Acad. Sci. US A* **114**, E8875–E8884
 45. Li, W., and Ye, Y. (2008) Polyubiquitin chains: functions, structures, and mechanisms. *Cell. Mol. Life Sci.* **65**, 2397–2406
 46. Gianni, M., Parrella, E., Raska, I., Jr., Gaillard, E., Nigro, E. A., Gaudon, C., Garattini, E., and Rochette-Egly, C. (2006) P38MAPK-dependent phosphorylation and degradation of SRC-3/AIB1 and RARalpha-mediated transcription. *EMBO J.* **25**, 739–751
 47. Uchida, S., Yoshioka, K., Kizu, R., Nakagama, H., Matsunaga, T., Ishizaka, Y., Poon, R. Y. C., and Yamashita, K. (2009) Stress-activated mitogen-activated protein kinases c-Jun NH2-terminal kinase and p38 target Cdc25B for degradation. *Cancer Res.* **69**, 6438–6444
 48. Hasler, U., Mordasini, D., Bens, M., Bianchi, M., Cluzeaud, F., Rousselot, M., Vandewalle, A., Feraïlle, E., and Martin, P. Y. (2002) Long term regulation of aquaporin-2 expression in vasopressin-responsive renal collecting duct principal cells. *J. Biol. Chem.* **277**, 10379–10386
 49. Puliyaanda, D. P., Ward, D. T., Baum, M. A., Hammond, T. G., and Harris, H. W., Jr. (2003) Calpain-mediated AQP2 proteolysis in inner medullary collecting duct. *Biochem. Biophys. Res. Commun.* **303**, 52–58
 50. Woelk, T., Oldrini, B., Maspero, E., Confalonieri, S., Cavallaro, E., Di Fiore, P. P., and Polo, S. (2006) Molecular mechanisms of coupled monoubiquitination. *Nat. Cell Biol.* **8**, 1246–1254
 51. Nemeth, E. F. (2002) The search for calcium receptor antagonists (calcilytics). *J. Mol. Endocrinol.* **29**, 15–21
 52. Kim, J. E., Jung, H. J., Lee, Y. J., and Kwon, T. H. (2015) Vasopressin-regulated miRNAs and AQP2-targeting miRNAs in kidney collecting duct cells. *Am. J. Physiol. Renal Physiol.* **308**, F749–F764
 53. Graca, J. A., Schepelmann, M., Brennan, S. C., Reens, J., Chang, W., Yan, P., Toka, H., Riccardi, D., and Price, S. A. (2016) Comparative expression of the extracellular calcium-sensing receptor in the mouse, rat, and human kidney. *Am. J. Physiol. Renal Physiol.* **310**, F518–F533
 54. Riccardi, D., and Brown, E. M. (2010) Physiology and pathophysiology of the calcium-sensing receptor in the kidney. *Am. J. Physiol. Renal Physiol.* **298**, F485–F499
 55. Huntzinger, E., and Izaurralde, E. (2011) Gene silencing by microRNAs: contributions of translational repression and mRNA decay. *Nat. Rev. Genet.* **12**, 99–110
 56. Gong, Y., Renigunta, V., Himmerkus, N., Zhang, J., Renigunta, A., Bleich, M., and Hou, J. (2012) Claudin-14 regulates renal Ca⁺⁺ transport in response to CaSR signalling via a novel microRNA pathway. *EMBO J.* **31**, 1999–2012
 57. Hasler, U., Leroy, V., Martin, P. Y., and Feraïlle, E. (2009) Aquaporin-2 abundance in the renal collecting duct: new insights from cultured cell models. *Am. J. Physiol. Renal Physiol.* **297**, F10–F18
 58. Tamma, G., Wiesner, B., Furkert, J., Hahm, D., Oksche, A., Schaefer, M., Valenti, G., Rosenthal, W., and Klusmann, E. (2003) The prostaglandin E₂ analogue sulprostone antagonizes vasopressin-induced antidiuresis through activation of Rho. *J. Cell Sci.* **116**, 3285–3294
 59. Maiti, A., Hait, N. C., and Beckman, M. J. (2008) Extracellular calcium-sensing receptor activation induces vitamin D receptor levels in proximal kidney HK-2G cells by a mechanism that requires phosphorylation of p38alpha MAPK. *J. Biol. Chem.* **283**, 175–183
 60. Yarova, P. L., Stewart, A. L., Sathish, V., Britt, R. D., Jr., Thompson, M. A., P. Lowe, A. P., Freeman, M., Aravamudan, B., Kita, H., Brennan, S. C., Schepelmann, M., Davies, T., Yung, S., Cholisoh, Z., Kidd, E. J., Ford, W. R., Broadley, K. J., Rietdorf, K., Chang, W., Bin Khayat, M. E., Ward, D. T., Corrigan, C. J., T. Ward, J. P., Kemp, P. J., Pabelick, C. M., Prakash, Y. S., and Riccardi, D. (2015) Calcium-sensing receptor antagonists abrogate airway hyperresponsiveness and inflammation in allergic asthma. *Sci. Transl. Med.* **7**, 284ra260
 61. Tfelt-Hansen, J., Yano, S., John Macleod, R., Smajilovic, S., Chattopadhyay, N., and Brown, E. M. (2005) High calcium activates the EGF receptor potentially through the calcium-sensing receptor in Leydig cancer cells. *Growth Factors* **23**, 117–123
 62. Krol, J., Loedige, I., and Filipowicz, W. (2010) The widespread regulation of microRNA biogenesis, function and decay. *Nat. Rev. Genet.* **11**, 597–610
 63. Murer, L., Addabbo, F., Carmosino, M., Procino, G., Tamma, G., Montini, G., Rigamonti, W., Zucchetta, P., Della Vella, M., Venturini, A., Zacchello, G., Svelto, M., and Valenti, G. (2004) Selective decrease in urinary aquaporin 2 and increase in prostaglandin E₂ excretion is associated with postobstructive polyuria in human congenital hydronephrosis. *J. Am. Soc. Nephrol.* **15**, 2705–2712
 64. Abdullah, H. I., Pedraza, P. L., McGiff, J. C., and Ferreri, N. R. (2008) Calcium-sensing receptor signaling pathways in medullary thick ascending limb cells mediate COX-2-derived PGE₂ production: functional significance. *Am. J. Physiol. Renal Physiol.* **295**, F1082–F1089
 65. Sansoè, G., Aragno, M., Tomasinelli, C. E., di Bonzo, L. V., Wong, F., and Parola, M. (2010) Calcium-dependent diuretic system in preascitic liver cirrhosis. *J. Hepatol.* **53**, 856–862
 66. Khositseth, S., Charngkaew, K., Boonkrai, C., Somparn, P., Uwathya, P., Chomane, N., Payne, D. M., Fenton, R. A., and Pisitkun, T. (2017) Hypercalcemia induces targeted autophagic degradation of aquaporin-2 at the onset of nephrogenic diabetes insipidus. *Kidney Int.* **91**, 1070–1087

Received for publication May 5, 2017.

Accepted for publication November 27, 2017.

THE
FASEB JOURNAL

The Journal of the Federation of American Societies for Experimental Biology

CaSR signaling down-regulates AQP2 expression *via* a novel microRNA pathway in pendrin and NaCl cotransporter knockout mice

Marianna Ranieri, Kamyar Zahedi, Grazia Tamma, et al.

FASEB J published online December 6, 2017

Access the most recent version at doi:[10.1096/fj.201700412RR](https://doi.org/10.1096/fj.201700412RR)

Subscriptions Information about subscribing to *The FASEB Journal* is online at
<http://www.faseb.org/The-FASEB-Journal/Librarian-s-Resources.aspx>

Permissions Submit copyright permission requests at:
<http://www.fasebj.org/site/misc/copyright.xhtml>

Email Alerts Receive free email alerts when new an article cites this article - sign up at
<http://www.fasebj.org/cgi/alerts>



Avanti
POLAR LIPIDS, INC.

Dive into lipidomics with
SPLASH™ Lipidomix® Mass Spec Standard*

*Includes all major lipid classes in ratios relative to human plasma